catalysts

MDPI

Article

Photodegradation of Herbicide Imazapyr and Phenol over Mesoporous Bicrystalline Phases TiO_2: A Kinetic Study

Mohamed Faycal Atitar [1], Adel. A. Ismail [2,3,*], Ralf Dillert [1] and Detlef W. Bahnemann [1,4,*]

1 Institut für Technische Chemie, Leibniz Universität Hannover, Callinstrasse 3, D-30167 Hannover, Germany
2 Nanotechnology and Advanced Materials Program, Energy & Building Research Center, Kuwait Institute for Scientific Research (KISR), P.O. Box 24885, Safat 13109, Kuwait
3 Central Metallurgical Research and Development Institute (CMRDI), P.O. 87 Helwan, Cairo 11421, Egypt
4 Laboratory of Photoactive Nanocomposite Materials, Department of Photonics, Faculty of Physics, Saint-Petersburg State University, Ulianovskaia str. 3, Peterhof, Saint-Petersburg 198504, Russia
* Correspondence: aaismail@kisr.edu.kw (A.A.I.); bahnemann@iftc.uni-hannover.de (D.W.B.); Tel.: +965-2498-9516 (A.A.I.); +49-511-762-5560 (D.W.B.)

Received: 10 July 2019; Accepted: 23 July 2019; Published: 27 July 2019

Abstract: Mesoporous TiO_2 nanoparticles were synthesized at different temperatures (400–800 °C). The resulting mesoporous anatase–rutile TiO_2 mixtures between 27 and 82% were found to have different structural properties (morphology, mesoporosity, crystallite phases, and sizes) affected through the calcination process. They were tested for the photocatalytic degradation of the herbicides imazapyr and phenol, compared with the nonporous TiO_2 P-25. The present work is an extension of a previously published study discussing the influence of the rutile content on the photocatalytic performance of the nanocrystals, based on the modified first order kinetic model, where the degradation rate is a function of the specific surface area of the material. The apparent degradation rate using T-800 is 10-fold higher than in the case using TiO_2 P-25. The material with the lowest anatase content (T-800) exhibits the highest photocatalytic activity in terms of initial reaction rate per unit surface area. It is considered that mixed-phase photocatalysts with rutile–anatase exhibit enhanced photoactivity with the increase of the rutile proportion.

Keywords: bicrystalline TiO_2; mesoporous TiO_2; photodegradation; kinetic model; imazapy; phenol

1. Introduction

TiO_2 photocatalyst, in its different forms and polymorphs, has attracted more attention in the past decades owing to its applications to environmental purification of polluted water and air, the development of self-cleaning super-hydrophilic surfaces, and the conversion and/or production of energy [1–3]. The elementary steps, which occur during the photocatalytic process, can illustrate its complexity. The analysis of these elementary reactions [4] as well as the kinetic relevance have been recognized, in the former research on TiO_2 photocatalysis, to reveal comprehensively the mechanism of electron transfer to/from bulk or surface species [5]. Furthermore, TiO_2 exists as two main polymorphs: anatase, a metastable phase, and rutile, a thermodynamically stable phase, with band gaps of 3.2 and 3.0 eV, respectively [6,7]. Several studies dealing with titanium dioxide phases (i.e., anatase and rutile) have been performed [8,9]. It has been reported that anatase is more photocatalytically active than rutile, which is the stronger photoabsorber. In addition to that, mixed phase TiO_2 (i.e., anatase and rutile), such as TiO_2 P-25, has been shown to be more effective than either pure anatase or rutile phase TiO_2 [6,10]. The improved performance of this mixed phase photocatalyst is attributed to a synergistic charge transfer across the anatase–rutile interface, although the mechanism of electron

transfer between the different phases (anatase and rutile) is still not clearly understood. This is due to the long-established controversy concerning the energetic alignment of the band edges of the rutile and anatase polymorphs [11]. However, the required proportions of these phases for the optimum photocatalytic activity are still a matter of debate because of the different synthesis pathways [12–15], crystallite sizes, and interactions between phases. Furthermore, insights into the influence of the photocatalyst type, i.e., form and amorphous, and reactivity on the mechanisms of the photocatalytic transformation are also based on the kinetic relevance. This has been done through the analysis of the reaction rate as a function of several operational parameters. In addition to that, such analysis is often a comparison of the reaction rate or quantum yield of various photocatalysts. Bahnemann et al. [16] recently reported about good practical methods to do such comparisons. Additionally, several studies correlated the photoactivity of TiO_2 with morphological aspects, especially the mesoporous structures, which showed the ability to enhance photocatalytic activity [17–22].

Recently, we have reported the synthesis, structural properties, and photocatalytic activities of mesoporous TiO_2 nanocrystals calcined at temperatures between 400 and 800 °C, resulting in a decrease in the anatase/rutile ratio with increasing calcination temperature [23]. The authors claimed that mesoporous TiO_2 calcined at 500 °C had the highest volumetric degradation rate for both imazapyr and phenol photocatalytic degradation. This was explained through the ordered mesoporous structure and the morphology, both of which helped to accumulate a higher amount of $^{\cdot}OH$ radicals inside the pores, and facilitate the transport and diffusion of the pollutants to the active site of the mesoporous TiO_2. However, it will be shown that the use of the volumetric degradation rate as a measure of photocatalytic activity of a material might result in misguiding interpretations. In this contribution, the photocatalytic activity was tested in the photodegradation of the herbicide imazapyr and phenol, based on the modified first order kinetic model, where the degradation rate is a function of the specific surface area of the material. The photocatalytic activity of the mesoporous materials was evaluated by comparison with the commercially available TiO_2 P-25. The latter is known to consist of 20% rutile and 80% anatase.

2. Results

The materials were characterized by means of several techniques as mentioned above (i.e., XRD, UV–vis, BET, Raman, and TEM) in previously publications [23]. The XRD patterns as well as Raman spectra revealed that all synthesized materials were a mixed phase TiO_2 (i.e., anatase/rutile). Among others, the sample T-400 showed very low crystallinity due to the incomplete transition from amorphous to anatase/rutile mixture. The low-temperature calcination step frequently results in amorphous or poorly crystallized titania with a high surface area [24]. For the other samples, the increase of the rutile content was found to be associated with the increase of the calcination temperature, i.e., the rutile content varied from 27 to 82%, while the calcination temperature increased from 500 to 800 °C, respectively. In contrast to that, Raman spectroscopy revealed the presence of mixed phase anatase/rutile through the typical Raman active modes of both anatase and rutile phases.

Furthermore, the BET surface area of the prepared TiO_2 nanocrystals ranged from 50 to 165 $m^2\ g^{-1}$, and the pore diameter ranged from 8.15 to 18.50 nm. For the T-800 sample, the results showed that this sample was non-porous, whereas the agglomeration of the formed large (nano) particles could be regarded as irregular voids between the particles. However, some mesoporosity was particularly evident from the TEM images (Figure 1). More relevant details about the characterization of the materials can be found elsewhere [23]. Table 1 summarizes the relevant data obtained from the characterization of the materials.

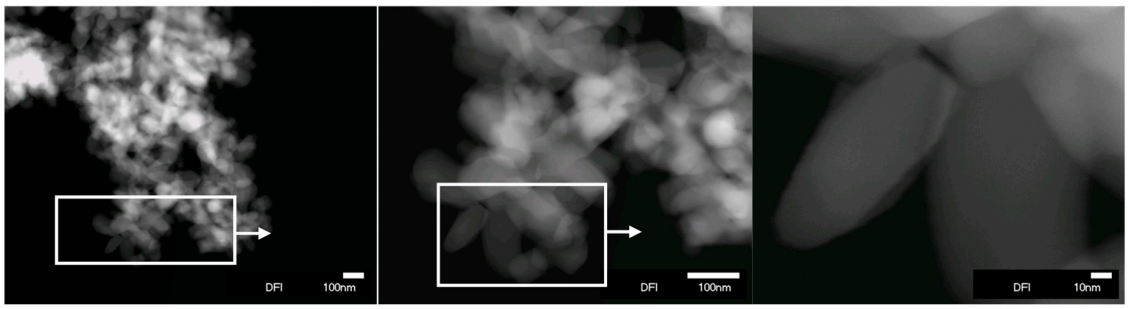

Figure 1. HRTEM images of the T-800 sample calcined at 800 °C.

The photocatalytic performance of the prepared mesoporous TiO_2 nanocrystals calcined at temperatures between 400 and 800 °C was evaluated using imazapyr and phenol as the probe molecules, and was compared to that of the commercial P-25 (Figure 2). All the newly prepared photocatalysts were found to be photocatalytically active. Both the photolytic degradation of an aqueous solution of the probe molecule and the elimination of the pollutant through dark adsorption on the photocatalyst surface, were performed as blank experiments [23]. The results indicate that the decomposition by homogeneous photoreaction in the absence of a photocatalyst as well as the removal by dark adsorption was negligible.

Assuming first-order kinetics, the rate constants of the degradation were calculated from the slope of the corresponding linear plot to Equation (1), and subsequently used to calculate the apparent degradation rate using the new expression Equation (5). The calculated apparent rate constants k_{app} for imazapyr as well as phenol photodegradation are summarized in Table 1.

$$\ln[C] = \ln[C_0] - k_{app} \times t \tag{1}$$

The kinetics of photocatalytic reactions at constant irradiance is usually described by a Langmuir–Hinshelwood-type rate law:

$$r_V = \frac{k_V K c}{1 + Kc} \tag{2}$$

with r_V, k_V, K, and c being the volumetric reaction rate, the maximum volumetric reaction rate, a parameter reflecting the adsorption of the respective probe molecule at the photocatalyst surface, and the molar concentration of the probe molecule, respectively. However, photocatalytic reactions are assumed to be reactions of adsorbed molecules. Therefore, a comparison of photocatalysts having different surface areas based on the volumetric reaction rate, i.e., the reaction rate per unit volume, will result in misguiding interpretations. In such a case the comparison has to be made on the basis of reaction rates per unit surface area.

In the case of a batch reactor,

$$V r_V = A r_A \tag{3}$$

holds with the assumption that the whole photocatalyst surface area A being present in the whole volume V of the suspension is the product of the BET surface area A_{BET} (in area per unit mass of photocatalyst), and the mass m_c of the photocatalyst in the reacting suspension (in mass of photocatalyst per unit volume of suspension) Equation (3) reads after insertion of Equation (2) and rearrangement

$$r_A = \frac{V}{A_{BET} m_c} \times \frac{k_V K c}{1 + Kc}. \tag{4}$$

In the case that $Kc < 1$ holds, Equation (4) simplifies into

$$r_A = \frac{V}{A_{BET} m_c} k_{app} c \tag{5}$$

with the apparent rate constant $k_{app} = k_V K$.

Figure 3 summarizes the calculated apparent degradation rate of imazapyr and phenol using the synthesized TiO_2 nanoparticles compared to the commercial P-25. First, it is assumed that, despite its high surface area, the low-temperature calcined sample T-400 contains amorphous or poorly crystallized titania [24]. Therefore, the discussion will focus mainly on the samples calcined between 500 and 800 °C. For imazapyr removal (Figure 3a), the results revealed that the apparent degradation rate increased in the order T-400 < T-500 < T-600 < T-700 < T-800, that is, in order of increase of the calcination temperature.

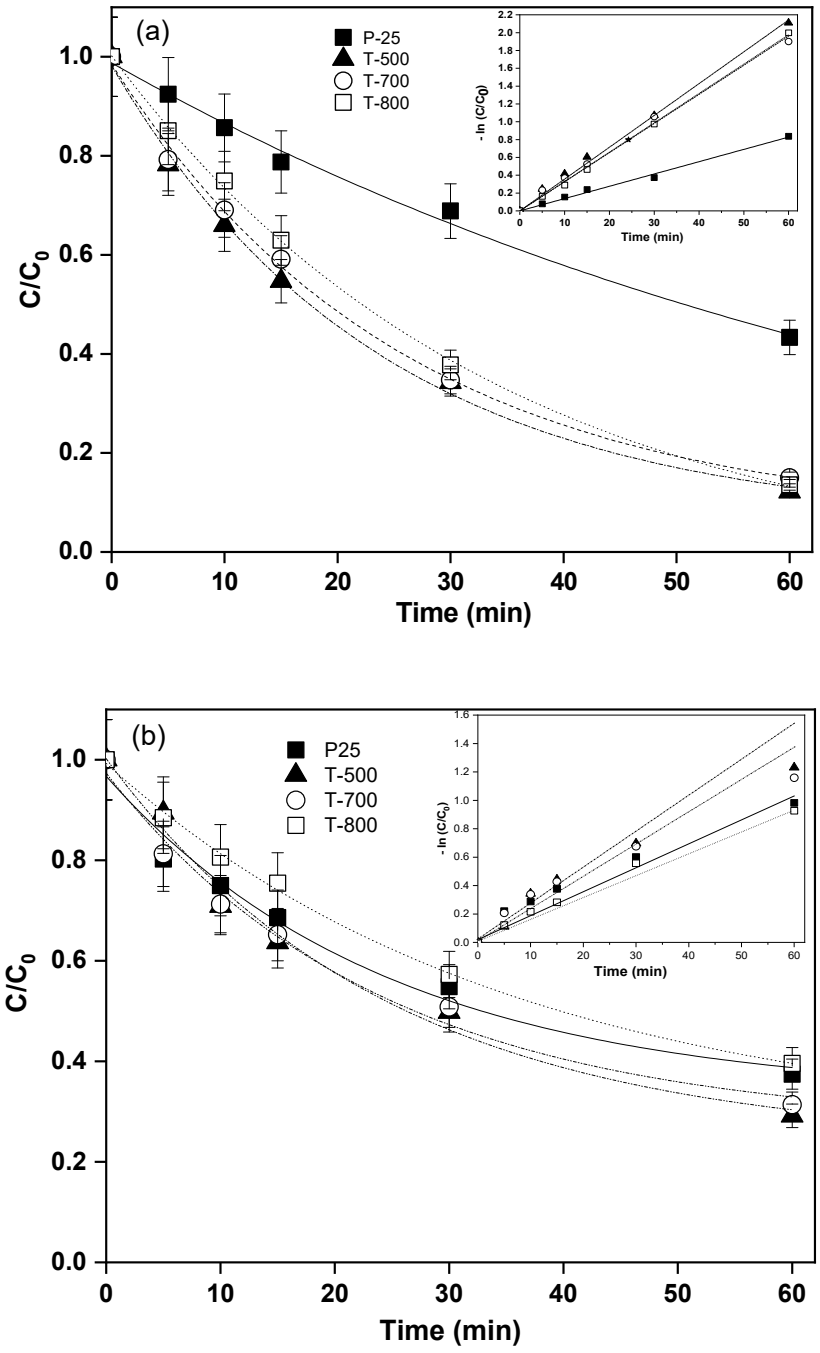

Figure 2. Change of the imazapyr (**a**) and phenol (**b**) concentration as a function of the illumination time using P-25, T-500, T-700, and T-800 photocatalysts. Insets are the linear fitting of the first order kinetics. Photocatalyst loading, 1 g L^{-1}; (O_2 saturated, pH = 3; T = 25 ± 1 °C); reaction volume 50 mL.

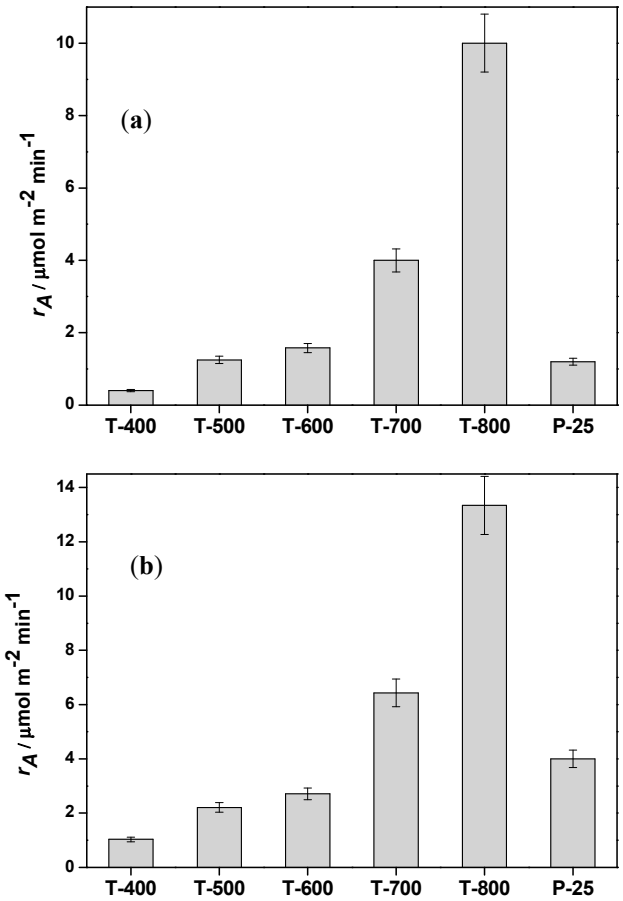

Figure 3. Comparison of the apparent degradation rate in the presence of commercial P-25, T-400, T-500, T-600, T-700, and T-800 photocatalysts for imazapyr (**a**) and for phenol (**b**). Photocatalyst loading, 1 g L^{-1}; (O_2 saturated, pH = 3; T = 25 ± 1 °C); reaction volume 50 mL.

As seen in Figure 3a, it is obvious that the T-800 significantly outperformed the T-500 despite having around 8-fold less surface area (Table 1). The apparent degradation rate using T-800 was approximately 10-fold higher than in the case using Aeroxide TiO_2 P-25, whereas the apparent degradation rates using P-25 and T-500 were almost equal. These two samples had different surface area but approximately the same anatase/rutile ratio, but differed in the porosity. It is concluded that the phase transformation, in this case from anatase to rutile, and the morphology of the sample (i.e., crystallinity, particle size, and porosity) resulting from the effect of calcination temperature were playing the major role in the improvement of the photocatalytic activity of the prepared samples.

Table 1. Textural properties of mesoporous TiO_2 calcined at 400 °C, 500 °C, 600 °C, 700 °C, and 800 °C and commercial P-25 and their photocatalytic performances.

Sample	Anatase (%)	Rutile (%)	A_{BET}/m^{2}g^{-1}	k_{app}/min^{-1} (Imazapyr)	k_{app}/min^{-1} (Phenol)	$r_{A,0}$/µmol m^{-2} min^{-1} (Imazapyr)	$r_{A,0}$/µmol m^{-2} min^{-1} (Phenol)
T-400	54	46	165	0.0134	0.0136	0.40	1.03
T-500	73	27	120	0.0344	0.0199	1.25	2.21
T-600	52	48	70	0.024	0.0148	1.58	2.71
T-700	47	53	35	0.0313	0.0182	4.0	6.43
T-800	18	82	15	0.0335	0.0152	10	13.34
P-25	80	20	50	0.0136	0.0152	1.2	4.00

Experimental conditions: C (imazapyr) = 0.080 mmol L^{-1}, C (phenol) = 0.25 mmol L^{-1}, m_c = 1 g L^{-1}, V = 0.05 L, data for anatase and rutile content, as well as the BET surface area (and the apparent rate constants for imazapyr and phenol degradation) were taken from [23].

For phenol (Figure 3b), the trend was nearly the same as for imazapyr. The highest apparent degradation rate was observed for the T-800 sample. The increase of the calcination temperature from 500 to 800 °C resulted in increasing the apparent rate from 2.21 μmol m^{-2} min^{-1} to 13.34 μmol m^{-2} min^{-1}, respectively. The same behavior was observed for the samples calcined at 400, 500, and 600 °C, which had lower apparent reaction rates than P-25. This is notwithstanding the fact that they had higher surface area than P-25. In contrast to that, the samples calcined at 700 and 800 °C had a higher apparent reaction rate but lower surface area than P-25. These results are in accordance with experimental results published by Pichat et al. [24,25]. The authors showed that for removal of phenol, the decrease in the electron–hole recombination rate outweighed the decrease in surface area resulting from the sintering temperature. This clearly indicated that surface area was not the factor mainly determining the photocatalytic activity [24,26,27].

In contrast to that, all mesoporous samples had lower anatase content than P-25. The material with the lowest anatase content (T-800) exhibited the highest photocatalytic activity in terms of initial reaction rate per unit surface area, even though it is generally claimed that a higher amount of anatase content and a higher surface area are necessary for a higher photocatalytic activity of the mixed phase photocatalyst. The data presented in this work clearly indicated that these statements are not generalized. Here, the photocatalyst T-800 with the lower surface area and the smaller amount of anatase was found to exhibit the highest photocatalytic activity in terms of surface reaction rate. This was due to the high crystallinity of the sample resulting from the high sintering temperature. Furthermore, the T-800 was highly photoactive because of the presence of junctions among different polymorphic TiO_2 phases that enhanced the separation of the photogenerated electron–hole pairs [15]. Consequently, the electron–hole recombination rate also had a substantial impact on the overall photocatalytic process. Mixed phase TiO_2 photocatalysts have been reported to have significantly higher activity than single phase TiO_2, and this has been interpreted as due to electronic interactions between the anatase and rutile phases, improved charge carrier separation, possibly through the trapping of electrons in rutile, and the consequent reduction in electron–hole recombination, and highly active sites formed at the phase interfaces [8,24]. Another important parameter that could be responsible for this higher activity is the band alignment between rutile and anatase, which in turn influences the charge transfer from/to rutile or anatase phases. Scanlon et al. [11] combined theory and experiment for understanding the band alignment between rutile and anatase and demonstrated that the electron affinity of anatase is higher than rutile, and that the photogenerated electrons flow from rutile to anatase [11].

Furthermore, the role of the surface hydroxyl density has been often neglected even if the concentration of OH per surface unit is considered to play a key role in the photocatalytic processes [28]. Sclafani et al. [29] attributed the high activities of the rutile phase photocatalyst to its large amount of hydroxyl groups on the surface, and proposed that they might trap the holes in the valence band and enhance the chemisorption of O_2, the conduction band [29]. Another important effect is the high crystallinity of the sample T-800. It has been reported that the improved titania crystallinity is coupled with reduction of crystal defects acting as recombination centers [28]. In contrast to that, low crystallinity is coupled with high specific surface area values and increased concentration of surface defects [26]; the latter can act as hydroxyl group/water molecule adsorption sites. It is obvious that the high crystallinity of the T-800 sample results in better charge carrier separation and reduced electron–hole recombination. In general, despite having the same chemical composition, the differences in the coordination environments, and hence chemical bonding, of rutile- and anatase- structured TiO_2 result in very different activities. The relationship between the electron chemical potentials and crystal structure and size are here responsible for the high photoactivity of the material T-800. Subsequently this reduces the electron–hole recombination and increases the formation of surface

active centers. In addition to that, the morphology of the T-800 samples allows the facile transfer of the target molecule to the former active centers where the oxidation is supposed to take place.

To explore the interest of mesoporous TiO_2 and their potential, recycling of the prepared mesoporous TiO_2 calcinated at 800 °C was evaluated for photodegradation of imazapyr and phenol over mesoporous TiO_2 nanoparticles with repeated cycles up to five times (Figure 4). The results displayed that the photocatalytic performance of the prepared mesoporous TiO_2 was not affected and it was quite stable with slight reduction after being recycled five times for 60 min illumination time, suggesting an outstanding catalyst for potential applications. This clearly explains the significant distinguishing of mesoporous TiO_2 nanoparticles on the photodegradation efficiency, which can be interpreted by its large porosity and accessible surface areas.

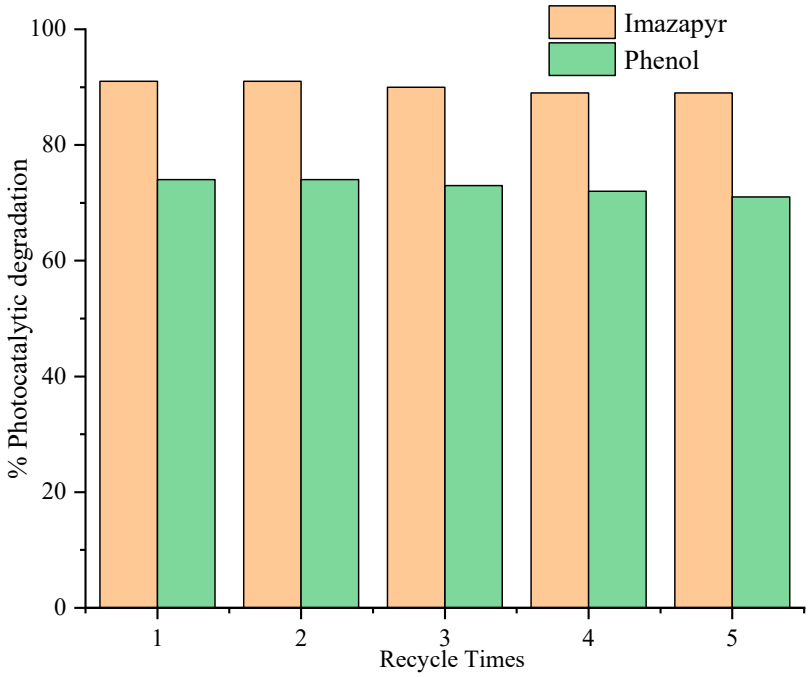

Figure 4. Repeated cycles up to 5 times for photodegradation of imazapyr and phenol over mesoporous TiO_2 nanoparticles. Illumination time, 60 min; photocatalyst loading, 1 g L^{-1}; pH = 3; T = 25 ± 1 °C; reaction volume 50 mL.

3. Materials and Methods

Mesoporous TiO_2 nanocrystals were prepared, as reported in detail [23], through a simple one step sol–gel process. Tetrabutylorthotitanate (TBOT) and F127 were used as precursor and structure directing agent, respectively. The obtained mesoporous TiO_2 nanocrystals were denoted as T-400, T-500, T-600, T-700, and T-800 related to the calcination temperatures.

The physical characterization of the newly prepared photocatalysts was carried out using X-ray diffraction, transmission electron microscopy (TEM), N_2 adsorption isotherms, Raman spectroscopy, as well as diffuse reflectance spectroscopy (DRS). More details about the instruments and the methods can be found elsewhere [23].

Imazapyr herbicide and phenol (Aldrich) were used as supplied. The experiments were carried out by adding the required quantity of TiO_2 (C_{cat} = 1 g L^{-1}) into 50 ml Pyrex flasks containing 10 mM KNO_3. The mixture was sonicated before use. The stirred suspensions were illuminated by means of a 1000 W Hg–Xe (Newport 6295NS) lamp equipped with a 10 cm water filter and dichroic beam turning mirror (66232 Newport Technology). The initial concentrations of the aqueous solutions of the organic pollutants was 0.08 mM for imazapyr and 0.27 mM for phenol. The pH of the solutions was adjusted to 3 since this pH value turned out to be optimal for the degradation of both pollutants. Control experiments were carried out in the absence of the photocatalyst (photolysis) as well as in

the absence of light (adsorption). Samples were taken out at regular time intervals. The analysis of concentration was carried out by means of high pressure liquid chromatography (HPLC).

4. Conclusions

The synthesized meso-structures were calcined at different temperatures to study their structural influence on the photocatalytic properties. The mesoporous TiO_2 photocatalysts are photocatalytically active, and show a higher activity for the decomposition of both imazapyr and phenol, compared to the commercially available Aeroxide TiO_2 P-25. The highest apparent degradation rate is observed for the T-800 sample. The increase of the calcinations temperature from 500 °C to 800 °C results in increasing the apparent rate from 2.21 μmol m^{-2} min^{-1} to 13.34 μmol m^{-2} min^{-1}, respectively. The mesoporous structure, the morphology, the crystal growth, and the phase transformation of the synthesized materials influence the photocatalytic activity. Therefore, it is concluded that the apparent degradation rate constant in term of specific area is useful to compare different photocatalysts with different surface areas. Additionally, evidence was found about the role of the rutile phase, which is considered to be enhanced the photocatalytic activity of the material.

Author Contributions: Conceptualization, M.F.A. and A.A.I.; methodology, M.F.A.; formal analysis and data curation, M.F.A., A.A.I., and R.D.; writing—original draft preparation, M.F.A., A.A.I., and R.D.; writing—review and editing, M.F.A., A.A.I., and R.D.; resources, D.W.B. and R.D.; supervision, D.W.B.

Funding: This research received no external funding.

Acknowledgments: M. F. Atitar gratefully acknowledges a scholarship from The German Academic Exchange Service (DAAD) in the Frame of a Sandwich-Program. A.A. Ismail acknowledges the Alexander von Humboldt (AvH) Foundation for granting him a renewed research fellowship. This work was supported by Saint-Petersburg State University via a research Grant ID 32706707. The publication of this article was funded by the Open Access Fund of the Leibniz Universität Hannover.

Conflicts of Interest: The authors declare no conflict of interest.

References

1. Tan, J.Z.Y.; Maroto-Valer, M.M. A review of nanostructured non-titania photocatalysts and hole scavenging agents for CO_2 photoreduction processes. *J. Mater. Chem. A* **2019**, *7*, 9368–9385. [CrossRef]
2. Schneider, J.; Matsuoka, M.; Takeuchi, M.; Zhang, J.; Horiuchi, Y.; Anpo, M.; Bahnemann, D.W. Understanding TiO_2 photocatalysis: Mechanisms and materials. *Chem. Rev.* **2014**, *114*, 9919–9986. [CrossRef]
3. Higashimoto, S. Titanium-dioxide-based visible-light-sensitive photocatalysis: Mechanistic insight and applications. *Catalysts* **2019**, *9*, 201. [CrossRef]
4. Friedmann, D.; Mendive, C.; Bahnemann, D. TiO_2 for water treatment: Parameters ffecting the kinetics and mechanisms of photocatalysis. *Appl. Catal. B Environ.* **2010**, *99*, 398–406. [CrossRef]
5. Minero, C.; Maurino, V.; Vione, D. Photocatalytic mechanisms and reaction pathways drawn from kinetic and probe molecules. In *Photocatalysis and Water Purification*; Wiley-VCH Verlag GmbH & Co. KGaA: Weinheim, Germany, 2013; pp. 53–72.
6. Khedr, T.M.; El-Sheikh, S.M.; Ismail, A.A.; Bahnemann, D.W. Highly efficient solar light-assisted TiO_2 nanocrystalline for photodegradation of ibuprofen drug. *Opt. Mater.* **2019**, *88*, 117–127. [CrossRef]
7. Khedr, T.M.; El-Sheikh, S.M.; Ismail, A.A.; Bahnemann, D.W. Photodegradation of 4-aminoantipyrine over nano-titania heterojunctions using solar and LED irradiation sources. *J. Environ. Chem. Eng.* **2019**, *7*, 102797. [CrossRef]
8. Hanaor, D.A.H.; Sorrell, C.C. Review of the anatase to rutile phase transformation. *J. Mater. Sci.* **2010**, *46*, 855–874. [CrossRef]
9. Bourikas, K.; Kordulis, C.; Lycourghiotis, A. Titanium dioxide (anatase and rutile): Surface chemistry, liquid-solid interface chemistry, and scientific synthesis of supported catalysts. *Chem. Rev.* **2014**, *114*, 9754–9823. [CrossRef]
10. Hurum, D.C.; Agrios, A.G.; Gray, K.A.; Rajh, T.; Thurnauer, M.C. Explaining the enhanced photocatalytic activity of Degussa P25 mixed-phase TiO_2 using EPR. *J. Phys. Chem. B* **2003**, *107*, 4545–4549. [CrossRef]

11. Scanlon, D.O.; Dunnill, C.W.; Buckeridge, J.; Shevlin, S.A.; Logsdail, A.J.; Woodley, S.M.; Catlow, C.R.A.; Powell, M.J.; Palgrave, R.G.; Parkin, I.P.; et al. Band alignment of rutile and anatase TiO_2. *Nat. Mater.* **2013**, *12*, 798–801. [CrossRef]
12. Shen, X.; Zhang, J.; Tian, B. Microemulsion-mediated solvothermal synthesis and photocatalytic properties of crystalline titania with controllable phases of anatase and rutile. *J. Hazard. Mater.* **2011**, *192*, 651–657. [CrossRef] [PubMed]
13. Fischer, K.; Gawel, A.; Rosen, D.; Krause, M.; Latif, A.A.; Griebel, J.; Prager, A.; Schulze, A. Low-temperature synthesis of anatase/rutile/brookite TiO_2 nanoparticles on a polymer membrane for photocatalysis. *Catalysts* **2017**, *7*, 209. [CrossRef]
14. Retamoso, C.; Escalona, N.; González, M.; Barrientos, L.; Allende-González, P.; Stancovich, S.; Serpell, R.; Fierro, J.L.G.; Lopez, M. Effect of particle size on the photocatalytic activity of modified rutile sand (TiO_2) for the discoloration of methylene blue in water. *J. Photochem. Photobiol. A Chem.* **2019**, *378*, 136–141. [CrossRef]
15. Bettini, L.G.; Dozzi, M.V.; Della Foglia, F.; Chiarello, G.L.; Selli, E.; Lenardi, C.; Piseri, P.; Milani, P. Mixed-Phase Nanocrystalline TiO_2 Photocatalysts Produced by Flame Spray Pyrolysis. *Appl. Catal. B Environ.* **2015**, *178*, 226–232. [CrossRef]
16. Kisch, H.; Bahnemann, D. Best practice in photocatalysis: Comparing rates or apparent quantum yields? *J. Phys. Chem. Lett.* **2015**, *6*, 1907–1910. [CrossRef] [PubMed]
17. Ismail, A.A.; Bahnemann, D. Metal-free porphyrin-sensitized mesoporous titania films For visible-light indoor air oxidation. *ChemSusChem* **2010**, *3*, 1057–1062. [CrossRef]
18. Robben, L.; Ismail, A.A.; Lohmeier, S.J.; Feldhoff, A.; Bahnemann, D.W.; Buhl, J.-C. Facile synthesis of highly ordered mesoporous and well crystalline TiO_2: Impact of different gas atmosphere and calcination temperatures on structural properties. *Chem. Mater.* **2012**, *24*, 1268–1275. [CrossRef]
19. Ismail, A.A.; Bahnemann, D.W.; Robben, L.; Yarovyi, V.; Wark, M. Palladium doped porous titania photocatalysts: Impact of mesoporous order and crystallinity. *Chem. Mater.* **2010**, *22*, 108–116. [CrossRef]
20. Ismail, A.A.; Bahnemann, D.W.; Bannat, I.; Wark, M. Gold nanoparticles on mesoporous interparticle networks of titanium dioxide nanocrystals for enhanced photonic efficiencies. *J. Phys. Chem. C* **2009**, *113*, 7429–7435. [CrossRef]
21. Ismail, A.A.; Bahnemann, D.W. One-step synthesis of mesoporous platinum/titania nanocomposites as photocatalyst with enhanced photocatalytic activity for methanol oxidation. *Green Chem.* **2011**, *13*, 428. [CrossRef]
22. Ismail, A.; Bahnemann, D. Mesostructured Pt/TiO_2 nanocomposites as highly active photocatalysts for the photooxidation of dichloroacetic acid. *J. Phys. Chem. C* **2011**, 5784–5791. [CrossRef]
23. Faycal Atitar, M.; Ismail, A.A.; Al-Sayari, S.A.; Bahnemann, D.; Afanasev, D.; Emeline, A.V. Mesoporous TiO_2 nanocrystals as efficient photocatalysts: Impact of calcination temperature and phase transformation on photocatalytic performance. *Chem. Eng. J.* **2015**, *264*, 417–424. [CrossRef]
24. Agrios, A.G.; Pichat, P. Recombination rate of photogenerated charges versus surface area: Opposing effects of TiO_2 sintering temperature on photocatalytic removal of phenol, anisole, and pyridine in water. *J. Photochem. Photobiol. A Chem.* **2006**, *180*, 130–135. [CrossRef]
25. Enríquez, R.; Agrios, A.G.; Pichat, P. Probing multiple effects of TiO_2 sintering temperature on photocatalytic activity in water by use of a series of organic pollutant molecules. *Catal. Today* **2007**, *120*, 196–202. [CrossRef]
26. Murakami, S.-Y.; Kominami, H.; Kera, Y.; Ikeda, S.; Noguchi, H.; Uosaki, K.; Ohtani, B. Evaluation of electron-hole recombination properties of titanium (IV) oxide particles with high photocatalytic activity. *Res. Chem. Intermed.* **2007**, *33*, 285–296. [CrossRef]
27. Bacsa, R.; Kiwi, J. Effect of rutile phase on the photocatalytic properties of nanocrystalline titania during the degradation of p-coumaric acid. *Appl. Catal. B Environ.* **1998**, *16*, 19–29. [CrossRef]
28. Di Paola, A.; Bellardita, M.; Palmisano, L.; Barbieriková, Z.; Brezová, V. Influence of crystallinity and OH surface density on the photocatalytic activity of TiO_2 powders. *J. Photochem. Photobiol. A Chem.* **2014**, *273*, 59–67. [CrossRef]
29. Sclafani, A.; Palmisano, L.; Schiavello, M. Influence of the preparation methods of TiO_2 on the photocatalytic degradation of phenol in aqueous dispersion. *J. Phys. Chem.* **1990**, *94*, 829–832. [CrossRef]